Journal of Materials and Electronic Devices 2 (2022) 26-33

Synthesis of Se doped CdO nanoparticles by sol-gel method, determination of structural and morphological properties

[1*]Cevher Kürşat Macit ,[2]Turan Gürgenc, [1]Cihan Özel

[1]Firat University, Engineering Faculty, Mechanical Engineering Department, Elazig, Turkey
[2]Firat University, Technology Faculty, Automotive Engineering Department, Elazig, Turkey

In this study, pure and Selenium (Se) doped Cadmium oxide (CdO) nanoparticles were synthesized by Sol-gel production method. Cadmium acetate dihydrate ($C_4H_6CdO4 \cdot 2H_2O$) was used as a cadmium source, and (Na_2SeO_3) was used as a selenium source. The structural and morphological properties of the synthesized nanoparticles were determined by Field Emission Scanning Electron Microscopy (FE-SEM), X-Ray Diffraction (XRD), Energy-dispersive X-ray spectroscopy (EDX) and Fourier Transform Infrared Spectroscopy (FT-IR) analyzes. As a result of the analysis, it was seen that Se doped CdO nanoparticles were produced successfully by sol-gel method. The produced nanoparticles are composed of almost spherical nanostructures. Particle sizes changed with Se doping and the smallest particle size was reached in the sample with 5% Se additive. The Se doping caused changes in unit cell volumes and crystal sizes of nanoparticles. The results show that the produced nanoparticles can be used in electronic devices containing semiconductor metal oxide.

Keywords: *Sol-gel, Selenium, CdO, Semiconductor, Nanomaterial.*

Submission Date: 29 March 2022
Acceptance Date: 21 May 2022

**Corresponding author: macitkursatcevher@gmail.com*

1. Introduction

Nanotechnology, which is the basic technology of the industrial period of today and the next centuries, is known as the science of controlling the atomic and molecular level of matter. In the simplest sense, nanotechnology, which is based on scientific determination and experience, has a very high contribution to the preservation of the world's liveability as a result of its contribution to the environment, energy, material durability and appropriate consumption. Today, high value-added technology is very important for business lines that require intense competition such as defense industry, pharmaceutical, automotive and textile applications. In recent years, nanotechnological discoveries have made significant progress, especially in materials science and many new products or processes in our lives. [1]. The materials used today have large-scale structures. Nano-structured materials that exhibit different and superior properties than these large-sized structures are called nanomaterials [2].

In order to produce nanomaterials, production methods that are different from the traditional production technologies used today are used. For this reason, different production methods from traditional production methods have been developed to be used in the nanotechnological field. By means of the developed production methods, structures with new physical, chemical and biological properties are obtained [3]. In recent years, significant progress has been made in the field of nanotechnology by utilizing II-VI semiconductor materials. Semiconductors, due to their high surface/volume ratio and quantum confinement effects, they have unique electronic, electrical, magnetic, optical and chemical properties in the nano-sized range. Because of these properties, semiconductors find their place in

applications such as phototransistors, sensors, diodes, low-emission windows, thin-film resistors, memory devices, and supercapacitors [4].

Considering the properties of CdO to be discussed in the study CdO compound is a II-IV group compound consisting of Cd, which is one of the second group elements of the periodic table, and O, which is the fourth group element. CdO is a transparent conductive oxide (TCO) material due to its high absorption and emission capacity. The band gap is between 2.2−2.7 eV, it is a direct band-pass and shows n-type conductivity. Its electrical conductivity is between $10^2 - 10^4$ S/cm. It was reported that the physical and chemical properties of CdO are relative to its stoichiometry as well as particle shape and size, which, in turn, depend on its preparation methods and preparation conditions [10,13,28,29,30,31,32]. CdO material is a suitable material for photodiodes, gas sensors, solar cells, phototransistors, anti-reflective coatings and IR detectors. Although Cd and its compounds are highly toxic, they are also used as key materials in battery production and to prevent corrosion in steel [14]. Electrical, optical, thermal and structural properties of CdO nanoparticles can be changed by doping metallic ions such as Ni, Al, Fe, Mn, Cr, La, In, Y, Tl, Sc, Sm, Dy and Ag to CdO [5].

The sizes and properties of nanoparticles may vary according to the preparation conditions and synthesis methods. Today, CdO nanoparticles can be synthesized by various methods such as sol-gel, spray pyrolysis, hydrothermal, chemical vapor deposition and chemical bath deposition [6-8]. The most important advantages of preparing nanoparticles using sol-gel are good chemical control of the composition, annealing at low temperature, homogeneity of the final product, adjusting the particle size and changing the morphology by changing the synthesis parameters [9-10]. The cytotoxic and photocatalytic properties of Se doped nickel oxide (NiO) nanoparticles were evaluated using the sol-gel synthesis method [11]. Se-doped SiO_2 nanocomposite material was produced by sol-gel synthesis method and its structural analysis and measurements were made [12]. The synthesis and structural characterization of $CuFeS_2$ and Se-doped $CuFeS_2$−xSex nanoparticles were investigated [16]. Improved photocatalytic activity and structural analyzes of Se-doped TiO_2 have been performed [17]. Structural, morphological and optical properties of Se-doped SnO_2 nanoparticles produced by sol-gel synthesis method were investigated [18]. Structural transition and improved phase transition properties of Se-doped G_2, Sb_2, Te_2 alloys were investigated [20].

After the literature research, it was seen that there was no research on the synthesis of Se-doped CdO nanoparticles by the Sol-Gel method, in our knowledge, and therefore it was decided to carry out the present study. In this study, pure and Se doped CdO nanoparticles in different mole percentages (mol.%) were synthesized by Sol-gel method. Structural and morphological characterization of the synthesized nanoparticles were investigated using FE-SEM, XRD and EDX analysis methods. The structural and morphological properties of nanoparticles were analyzed in detail.

2. Experimental

Cadmium acetate dihydrate ($C_4H_6CdO_4 \cdot 2H_2O$) and Sodium selenite (Na_2SeO_3) were used as sources of Cd and Se sources, respectively. Syntheses were performed according to the sample order given in Table 1. In the synthesis process, 0.5 M $C_4H_6CdO_4 \cdot 2H_2O$ was first added to 20 ml of methanol in a beaker and mixed in a magnetic stirrer until all particles dissolved (Mixture-1). In the other beaker, it was mixed until 2.5 M NaOH was dissolved in 20 ml of methanol (Mixture-2). Mixture-2 was slowly poured into mixture-1, so these two solutions were combined in one beaker. The resulting mixture solution was stirred at 80 °C for 2 hours. The solution was allowed to cool to room temperature. Then, the nanoparticles that collapsed with the filter paper were filtered and washed with alcohol. After washing with alcohol, rinsing was performed several times with distilled water. Nanoparticles were dried in an oven at 80 °C. The dried particles were grinded with a mortar and then annealed in an oven at 450 °C for 1 hour. Synthesis of Se-doped nanoparticles was also carried out in the same way. The only difference is that different mole percentages (1%, 5% and 10%) (Na_2SeO_3) were added to the mixture-1.

Table 1. Synthesized samples.

Sample	Content
1	Pure CdO
2	1% Se doped CdO
3	5% Se doped CdO
4	10% Se doped CdO

XRD and FT-IR analyzes were performed to characterize the functional groups and structural properties of the samples, respectively. PANalytical Empyrean was used for XRD analysis and Thermo Scientific Nicolet IS5 FT-IR spectrometer was used for FT-IR analysis. FT-IR analysis was performed at a scanning range of 4000-500 cm^{-1}. XRD analysis was performed in CuKα (λ = 1.5406 ˚A) radiation at 2θ = 20 to 90° scanning range and 40 kV/40 mA. The morphologies and chemical compositions of the synthesized pure and Se-doped nanoparticles were examined with Zeiss Sigma 300 brand emission FE-SEM and EDX analysis, respectively, and the particle sizes and the resulting doping ratios were investigated.

3. Results and Discussion

Fig.1 shows the macro images of the synthesized pure and Se-doped CdO nanoparticles. As the Se contribution on the samples was increased, the color change of the samples was clearly seen as a result of annealing. As the amount of Se increased, the colors of the synthesized samples became lighter.

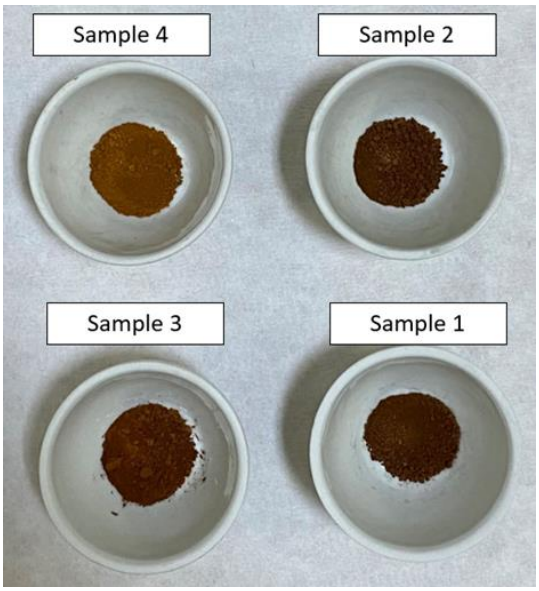

Fig.1. Synthesized samples.

High intensity peaks were used to determine the crystal sizes of the samples and the structural parameters of the samples were calculated using the following formulas. The following equation is used to find the distance (d) between two adjacent planes [15];

$$d = \frac{a}{\sqrt{(h+k+l)}} \quad (1)$$

where d is the distance between two adjacent planes and h, k and l are Miller indices. To calculate the crystal size of the samples, it was calculated using the Scherer equation given below [15];

$$D = \frac{0.9\lambda}{\beta cos\theta} \quad (2)$$

where λ is the wavelength of the X-ray in nm, β is the full width at half maximum in radians, and θ is the diffraction angle in degrees. The volumes of the unit cells (V) were calculated from the following equation [19,26];

$$V = a^3 \quad (3)$$

The FT-IR spectra of pure and Se-doped CdO nanoparticles synthesized by the Sol-Gel method are shown in Fig.2. The band intensities and positions were changed by the effect of Se doping on the CdO lattice [23]. These results show that the Se is doped appropriately to the CdO nanoparticles and the formation of the nanomaterial has taken place. According to the FT-IR results, the stretching occurring in the range of approximately 3000-3400 cm^{-1} is attributed to O-H [27]. The attributed O-H stretch is thought to result from water reabsorption during storage in ambient air [27]. In the 10% Se added sample, the effect of Se additive is observed in the range of 750-1000 cm^{-1} [23]. Due to the low contribution of Se in other samples, the contribution of Se could not be seen clearly in this region. The peaks occurring at approximately 614.21 cm^{-1}, 561.18 cm^{-1} and 549.61 cm^{-1} correspond to the presence of CdO stretching [27].

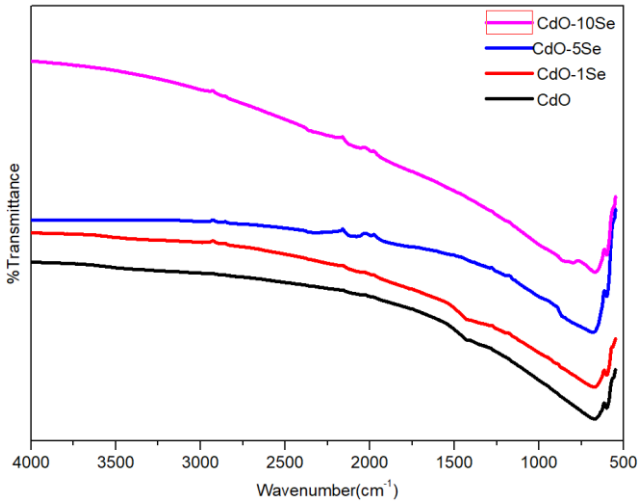

Fig.2. FT-IR analysis results of the synthesized samples.

The XRD diffraction results of pure and Se-doped CdO nanoparticles are shown in Figure 3. The 2θ values of the synthesized pure and Se-doped nanoparticles in different doping ratios are given in Table 2, and the calculated values of the diffraction planes, lattice parameters, unit cell volumes, crystal sizes and average crystal sizes are given in Table 3. Intense peaks corresponding to 2θ degrees of 33.132°, 38.437°, 55.401°, 66.037°, 69.372° and 82.134° in pure CdO sample are compatible with JCPDS card no. 78-0653 and literature studies. These peaks correspond to the cubic phase of CdO and are attributed to the planes (111), (200), (220), (311), (222) and (300), respectively. Although the peak positions and intensities of Se doped nanoparticles differ according to the Se doping ratio, they still match with the JCPDS card. no. 78-0653. In addition, as the Se doping ratio increased, the peak intensities increased. No secondary phases or impurities were found in pure, 1% mol. Se and 5% mol. 5% Se added samples. This shows that the samples are of high purity and single-phase structure. In addition, it was observed that Se contributes effectively to the CdO host lattice at 1% mol Se and 5% mol Se doping ratios, and Se particles show a good distribution on the CdO surface

[23,25]. On the other hand, in the highly Se doped sample (CdO-10Se), besides the characteristic peaks of CdO, SeO_2 peak at an angle of approximately 29.219°, 2θ were also observed [27]. It is thought that this is due to the increase in the amount of Se at this doping level. As the Se doping ratio increased, it was observed that the peaks shifted to slightly lower 2θ angles in the other samples, except for the 10% Se doped sample. This is because Se^{+4} ions are evenly distributed in the CdO lattice and due to different ionic radius (Cd^{+3}= 0.097nm > Se^{+4}= 0.064nm), a lattice distortion occurs and increases with the increase of Se doping [22]. It can be said that the variation in the 2θ angles is limited due to the low difference between the ionic radius. All of the calculated values were affected by the change in the Se doping ratio. Except for the CdO-10Se sample, which has the highest doping ratio, the lattice parameters and unit cell volumes of the other samples are slightly higher than that of pure CdO. As the doping ratio increased, these parameters increased even more. At high doping ratio, the lattice parameters and unit cell volume of the sample are the highest. In studies on CdO doped with different additives and at different ratios, differences were observed in lattice parameters and unit cell volumes [24,25,26]. The average crystal sizes of the Se doped samples are lower than the pure CdO sample and the lowest value is 27.6377 nm in the 5% Se doped sample. The unit cell volumes and lattice parameter values of nanoparticles decreased at 1%Se and 5%Se doping ratios, and increased at 10%Se doping ratio. XRD results reveal that pure and Se-doped CdO nanoparticles were successfully synthesized by sol-gel method.

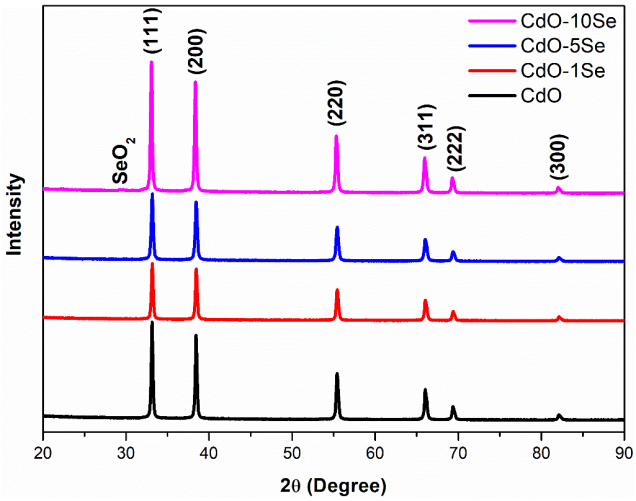

Fig.3. XRD analysis results of samples.

Table 2. 2θ values of synthesized samples.

Sample	CdO	CdO-1Se	CdO-5Se	CdO-10Se
(111)	33.132	33.158	33.159	33.053
(200)	38.437	38.463	38.437	38.332
(220)	55.401	55.427	55.427	55.322
(311)	66.037	66.037	66.010	65.958
(222)	69.372	69.372	69.372	69.293
(300)	82.134	82.134	82.082	82.029

Table 3. Calculated values of diffraction planes, lattice sizes, unit cell volumes, crystal sizes and average crystal sizes of the samples.

Sample	CdO	CdO-1Se	CdO-5Se	CdO-10Se
Diffraction Planes	111 200	111 200	111 200	111 200
2θ Diffraction Angles (degree)	33.132 38.437	33.158 38.463	33.159 38.437	33.053 38.332
a=b=c (Å)	4.6794	4.6759	4.6757	4.6903
V (Å^3)	102.466	102.231	102.223	103.181
Crystal Size (nm)	32.9569 31.5999	31.0981 30.2307	28.1333 27.1422	32.4774 31.1322
Average Crystal Size (nm)	32.2784	30.6644	27.6377	31.8048

FE-SEM images and EDX analysis results of pure and Se-doped CdO nanoparticles are shown in Fig. (4-7). The compositions of the elements in the synthesized nanoparticles are given in Table 4. The synthesized pure and Se-doped CdO particles are nanosized, and the morphology of the nanoparticles is almost spherical. The synthesized nanoparticles were agglomerated in places due to their high surface energies [5]. As seen from the EDX analysis, Se was found in the Se-doped samples and the Se ratio increased as expected as the doping ratio increased. Pure CdO nanoparticles were composed of 75.66% O, and 24.34% Cd. CdO-1Se nanoparticles were composed of 69.38% O, 30.03% Cd and 0.58% Se. CdO-5Se nanoparticles were consists of 69.53% O, 29.69% Cd and 0.79% Se. CdO-10Se nanoparticles were composed of 65.05% O, 33.97% Cd and 0.98% Se. This shows that the Se doping was successfully performed on CdO.

Table 4. Chemical compositions of samples.

Sample	Content (at.%)		
	O	**Cd**	**Se**
1	%75.66	%24.34	-
2	%69.38	%30.03	%0.58
3	%69.53	%29.69	%0.79
4	%65.05	%33.97	%0.98

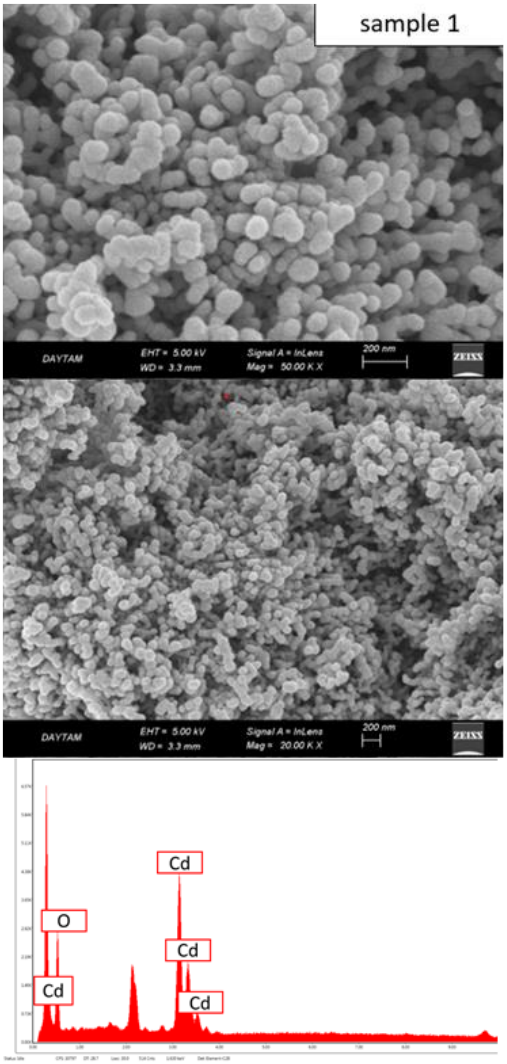

Fig.4. FE-SEM images and EDX analysis of CdO sample.

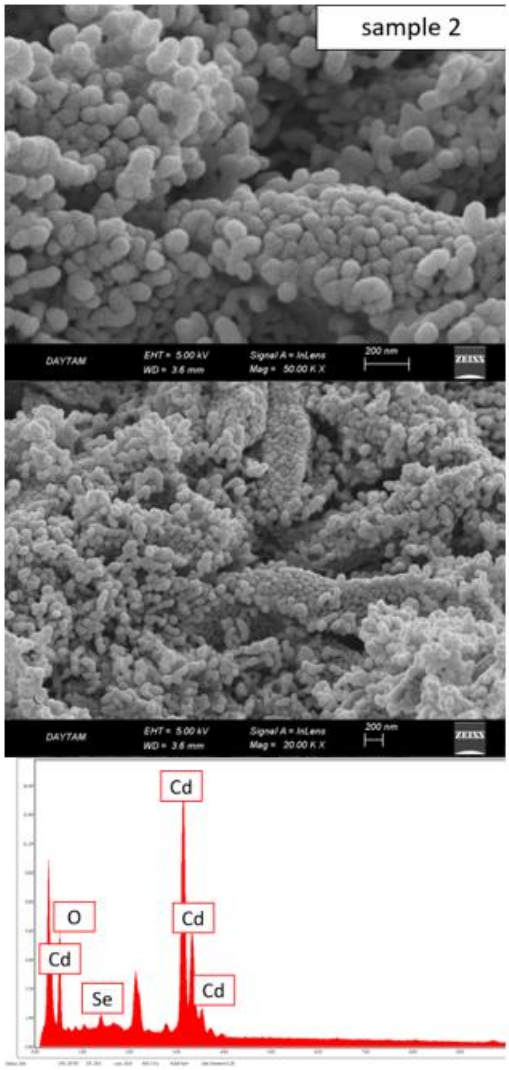

Fig.5. FE-SEM images and EDX analysis of CdO-1Se sample.

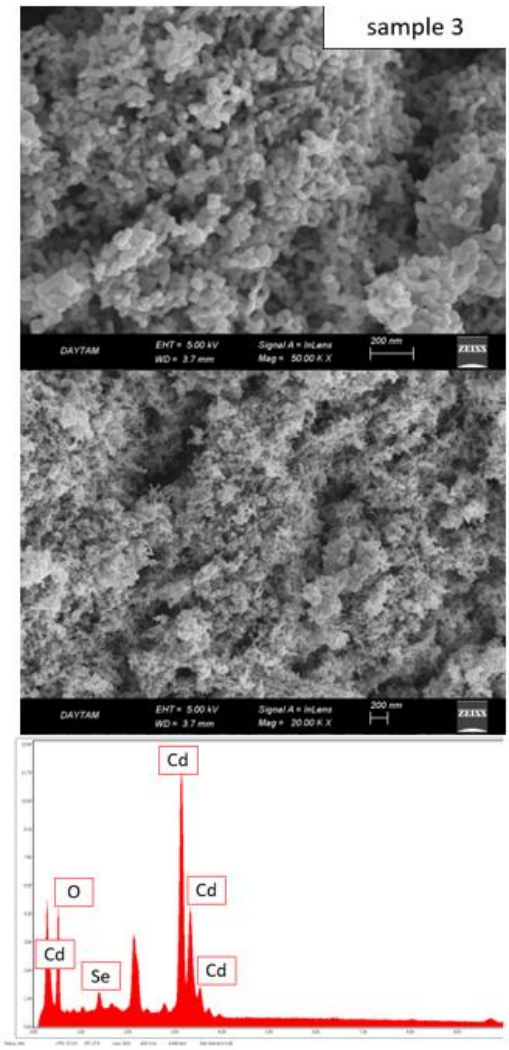

Fig.6. FE-SEM images and EDX analysis of CdO-5Se sample.

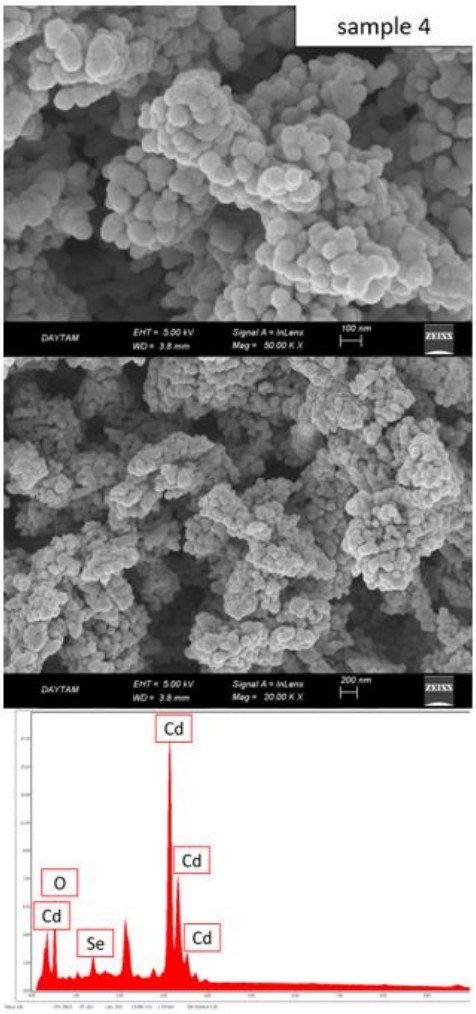

Fig.7. FE-SEM images and EDX analysis of CdO-10Se sample.

4. Conclusion

Pure and Se-doped CdO nanoparticles were successfully synthesized by sol-gel method. The synthesized particles are nanosized and have an almost spherical structure. The diffraction angles shifted with the increase of Se doping ratio. The structural and morphological properties of nanoparticles were affected by Se addition. The results show that the produced nanoparticles can find use in the semiconductor industry.

References

[1] M. Ersöz, A. Işıtan, M. Balaban Handbook of Fundamentals of Nanotechnology,Turkey, BilalOfset, 2018

[2] Z. Tüylek Nevşehir Journal of Science and Technology Vol. 5(2) 130-141 (2016)

[3] H. Ateş, Gazi University Journal of Science Part:C, Design and Technology GU J Sci Part:C 3(1):437-442 (2015)

[4] K. Mohanraj, D. Balasubramanian, J. Chandrasekaran, Bose A C. Mater. Sci. Semicond. Process. 2018; 79: 74-91.

[5] R. Bhargava, S. Khan, M. M. N. Ansari, N. Ahmad, Mater. Today: Proc. (2018); 5(9): 17636-17640.

[6] Mosquera E, del Pozo I, Morel M. Journal of Solid State Chemistry 206 (2013) 265–27 (2013)

[7] Tawfik W Z, Esmat M, El-Dek S. Appl Nanosci (2017) 7:863–870

[8] Yathisha R, Nayaka Y A, Manjunatha P, Vinay M, Purushothama H. Doping, Microchem. Microchemical Journal 145 (2019) 630–641631

[9] Sagadevan S, Veeralakshmi A. International Journal of Chemical and Molecular Engineering Vol:8, No:12, (2014)

[10] S. Reddy, B.E.K. Swamy 1, U. Chandra, B.S.Sherigara , H.Jayadevappa, Int. J. Electrochem. Sci., 5 (2010) 10 - 17

[11] S.Ghazala, A. Akbaria, H. A. Hosseinia , Z.Sabourib , M.Khatamic and M. Darroud ,Inorg. Chem. Res., Vol. 5, No. 1, 37-49, June 2021 DOI: 10.22036/icr.2020.258236.1094

[12] R. Durga devi a, A. Ganapathi, Materials Science for Energy Technologies 5 (2022) 161–170162

[13] W. Dong, C. Zhu, Opt. Mater, 22 (2003) 227

[14] Chandiramouli, R. ve Jeyaprakash, B. G. (2013). Solid State Sci. 16, 102-110.

[15] K. Mohanraja, D. Balasubramaniana, J. Chandrasekaranb, A. C. Bosec Materials Science in Semiconductor Processing 79 (2018) 74–91

[16] H. Yu, J. Xu, Y. Hu, H. Zhang, C. Zhang, C.Qiu· X.Wang, B. Liu, L. Wei1, J. Li, Journal of Materials Science: Materials in Electronics (2019) 30:12269–12274

[17] W. Xie, R. Li, Q. Xu Scientific Reports (2018) 8:8752 | DOI:10.1038/s41598-018-27135-4

[18] S.Kumar, P. Chauhan, V. Kundu, J Mater Sci: Mater Electron (2016) 27:3103–3108

[19] T. Oyama, S., Onkawa, T., Takagaki, A. *et TopCatal* **58,** 201–210 (2015).

[20] E. M. Vinod, K. Ramesh K. S. Sangunni Scientific Reports | 5: 8050 | DOI: 10.1038/srep08050

[21] S. E. Algarni, A. F. Qasrawi, Najla M. Khusayfan Applied Physics A (2022) 128:254

[22] A. S. Irfan, L. Li, A. Saleemi and C. Nan, J. Mater. Chem. A, 2017, DOI: 10.1039/C7TA01847A.

[23] P. Bhatia, S. Pandey, R. Prakash & T. P. Nagaraja (2014), Journal of Biologically Active Products from Nature, 4:5-6, 354-364, DOI: 10.1080/22311866.2014.961103

[24] Sivakumar S, Venkatesan A, Soundhirarajan P, Khatiwada C P. Synthesis, Spectrochimica Acta Part A: Molecular and Biomolecular Spectroscopy 136 (2015) 1751–1759

[25] E. Gürgenç, A. Dikici, F. Aslan," Journal Pre-proof S0921-4526(22)00300-3, (2022)

[26] E. Gürgenç, A. Dikici, F. Biryan, F. Aslan, K. Koran Fırat University Journal of Engineering Sciences 34(1), 229-237, 2022

[27] K. Mohanraja, D. Balasubramaniana, J. Chandrasekaranb, A. C. Bosec, Materials Science in Semiconductor Processing 79 (2018) 74–91

[28] C.H. Bhosale, A.V. Kambale, A.V. Kokate, Mater. Sci. Eng., B, Solid-StateMater. Adv. Technol, 122 (2005) 67.

[29] M. Ghosh, C.N.R. Rao, Chem. Phys. Lett, 393 (2004) 493.

[30] M. Ristić, S. Popović, S. Musić, Mater. Lett, 58 (2004) 2494.

[31] W. Shi, C. Wang, H. Wang, Cryst. Growth Des, 6 (2006) 915.

[32] 14. H. Yu, D. Wang, M. Han, J. Am. Chem. Soc, 129 (2007) 2333.